J. Fluid Mech. (1997), *vol.* 352, *pp.* 245–264. Printed in the United Kingdom

Free boundary effects on baroclinic instability

By F. J. BERON-VERA AND P. RIPA

Centro de Investigación Científica y de Educación Superior de Ensenada, Km. 107 Carretera Tijuana-Ensenada, (22800) Ensenada, B.C., México

(Received 17 September 1996 and in final form 23 July 1997)

The effects of a free boundary on the stability of a baroclinic parallel flow are investigated using a reduced-gravity model. The basic state has uniform density stratification and a parallel flow with uniform vertical shear in thermal-wind balance with the horizontal buoyancy gradient. A finite value of the velocity at the free (lower) boundary requires the interface to have a uniform slope in the direction transversal to that of the flow. Normal-mode perturbations with arbitrary vertical structure are studied in the limit of small Rossby number. This solution is restricted to neither a horizontal lower boundary nor a weak stratification in the basic state.

In the limit of a very weak stratification and bottom slope there is a large separation between the first two deformation radii and hence short or long perturbations may be identified:

(*a*) The short-perturbation limit corresponds to the well-known Eady problem in which case the layer bottom is effectively rigid and its slope in the basic state is immaterial.

(*b*) In the long-perturbation limit the bottom is free to deform and the unstable wave solutions, which appear for any value of the Richardson number *Ri*, are sensible to its slope in the basic state. In fact, a sloped bottom is found to stabilize the basic flow.

At stronger stratifications there is no distinction between short and long perturbations, and the bottom always behaves as a free boundary. Unstable wave solutions are found for $Ri \to \infty$ (unlike the case of long perturbations). The increase in stratification is found to stabilize the basic flow. At the maximum stratification compatible with static stability, the perturbation has a vanishing growth rate at all wavenumbers.

Results in the long-perturbation limit corroborate those predicted by an approximate layer model that restricts the buoyancy perturbations to have a linear vertical structure. The approximate model is less successful in the short-perturbation limit since the constraint to a linear density profile does not allow the correct representation of the exponential trapping of the exact eigensolutions. With strong stratification, only the growth rate of long enough perturbations superimposed on basic states with gently sloped lower boundaries behaves similarly to that of the exact model. However, the stabilizing tendency on the basic flow as the stratification reaches its maximum is also found in the approximate model. Its partial success in this case is also attributed to the limited vertical structure allowed by the model.

1. Introduction

The classical problem of baroclinic instability consists of the study of normal-mode perturbations to a parallel flow with uniform vertical shear in thermal-wind balance with a horizontal density gradient. The layer of fluid has uniform vertical

stratification and is confined between two horizontal rigid boundaries. This problem posed on a uniformly rotating frame is known as the Eady model (e.g. see Gill 1982 or Pedlosky 1987). Unstable quasi-geostrophic wave solutions in the Eady model correspond to a Richardson number $Ri \to \infty$. Stone (1966, 1970) investigated the non-geostrophic corrections to the Eady model. Analytic formulas for the corrections were derived in Stone (1966) and demonstrated to be in good agreement with the more exact numerical dispersion relations in Stone (1970). Three types of unstable wave solutions were isolated: one type was the conventional baroclinic instability (i.e. that of Eady extended to the ageostrophic regime) which dominated when $Ri \gtrsim 1$; the other two types, symmetric and Kelvin–Helmholtz instabilities, existed only when $Ri < 1$. It should be mentioned that the results published by Stone (1966, 1970) are not entirely correct since Kelvin–Helmholtz instability cannot arise when the basic current has a uniform vertical shear (Ripa 1990; Vanneste 1993).

More recently, Fukamachi, McCreary & Proehl (1995, hereinafter referred to as FMP), studied the stability of a baroclinic parallel current in an oceanic mixed layer and showed that the existence of a free boundary may result in a non-vanishing growth rate for the perturbations at all wavenumbers. FMP used a one-layer reduced-gravity model allowing for an arbitrary vertical structure for the perturbations as well as vertical displacements of the base of the active layer. The basic state had uniform vertical stratification, which was assumed weak, and a parallel flow with uniform vertical shear. According to the thermal-wind balance, a flow of such characteristics requires, in general, a uniform slope at the base of the active layer in the direction transversal to that of the flow. However, FMP's analysis was restricted to the particular situation in which the active layer's base is horizontal, which can be shown to correspond to a vanishing value of the velocity at the interface (since the deep layer is assumed at rest). FMP derived an analytic expression for the dispersion relation (valid for low-frequency, low-wavenumber waves) assuming $Ri \sim 1$, and concluded that all wavenumbers were unstable. FMP also computed numerical solutions restricted to neither low-frequency nor low-wavenumber waves, and using a minimum value for $Ri = 1$ in order to avoid the presence of symmetric and Kelvin–Helmholtz instabilities. (Kelvin–Helmholtz instability is, however, excluded from this problem, even if $Ri < 1$, as stated above.) The numerical solution corroborated the analytic result and extended its range of validity. The instabilities found in the numerical calculation followed the functional dependence on Ri suggested by Stone (1966). In consequence, FMP argued that the unstable wave solutions derived analytically were a manifestation of non-geostrophic baroclinic instability.

FMP also compared results with those predicted by an approximate layer model that allows for density variations in time and horizontal position but keeps all dynamical fields as depth independent, finding only minor differences between the dispersion relations provided by both models. These 'slab' models have been extensively exploited (see Ripa 1996*a* and references therein). They represent an approximation and do not have an explicit representation of the vertical shear, which, for instance, is associated with horizontal buoyancy gradients (through the thermal-wind balance). An improvement of these primitive equations models, proposed by Ripa (1995, hereinafter referred to as R95), uses velocity and buoyancy fields varying linearly with depth. The slab model and the new one are denoted by IL^0PEM and IL^1PEM respectively, since they are the first and second truncations of an exact inhomogeneous layer primitive equations model, indicated by IL^∞PEM. Thus the superscript n in IL^n indicates the amount of vertical variation allowed for the density field in the sense of the degree of polynomials in depth. The IL^1PEM is able to represent explicitly

the thermal-wind balance at low frequencies. Its quasi-geostrophic version, called IL^1QGM, was developed in Ripa (1997*a*, hereinafter referred to as R97).

The subinertial mixed layer (SML) approximation of Young (1994) is another attempt to cure the deficiencies of the slab models. It has a free parameter $\mu := |f|^{-1}/\tau_U$, where τ_U is the time scale for vertical mixing of momentum and $|f|^{-1}$ is the inertial time scale, f being the Coriolis parameter. For $\mu \to \infty$ Young's model coincides with the IL^0QGM (Ripa 1996*b*), whereas for $\mu \to 0$ it has an implicit representation of the velocity's vertical shear (through the thermal-wind balance) and therefore it is not quite the same as the IL^1QGM.

In R97 a comparison is presented of the approximate models (IL^0, SML and IL^1) and the exact one (IL^∞) in the sense of the free waves superimposed on a motionless reference state and the integrals of motion. Let the constants H_r, g_r and N_r be the depth, mean buoyancy (relative to the lower layer) and Brunt–Väisälä frequency in that state. Two independent horizontal scales can be defined, namely

$$R_E := \frac{(g_r H_r)^{1/2}}{|f|} \quad \text{and} \quad R_I := \frac{N_r H_r}{|f|}. \tag{1.1}$$

For each horizontal wavenumber, the IL^∞ model sustains an infinite set of Rossby waves, corresponding to the vertical modes of the system. For weak stratification ($R_I \ll R_E$), the 'equivalent barotropic' or external mode has a deformation radius R_E, whereas the internal modes have radii $R_I/(n\pi)$ ($n = 1, 2, ...$). The approximate models have only a finite number of those vertical modes: three in the case of the IL^1 (with radii equal to $R_E, R_I/\sqrt{12}$ and 0) and two for the IL^0 and the SML models (with radii equal to R_E and 0). A vanishing deformation radius corresponds to a zero-frequency Rossby wave or 'force compensating mode' (R95; Ripa 1996*a*; R97). This has zero or negative free energy in the IL^0 or SML models respectively, whereas all modes have positive energy for both the IL^1 and IL^∞ models.

The approximate models (IL^0, SML and IL^1) were also compared in R97 for the baroclinic instability problem in the limit of weak stratification $R_I/R_E \to 0$. That comparison is completed here with the derivation of the dispersion relation and structure of the normal modes for the IL^∞ model in the case of perturbations with wavelengths of $O(R_E)$. FMP's horizontal bottom constraint for the basic state is relaxed and shown to have important dynamic effects on its stability. The analysis is also extended to arbitrary stratifications in the basic state, i.e. R_I and R_E of the same order. All these calculations correspond to including free boundary effects to the classical Eady problem. The study is carried out within the realm of a low-frequency approximation: a Rossby number perturbation expansion is applied to the IL^∞PEM and the IL^1QGM is used.

The rest of this paper is organized as follows. The IL^∞PEM is presented in §2 together with a review of the derivation of the IL^1PEM and its low-frequency approximation IL^1QGM. A comparison of the results from the normal modes baroclinic stability analysis corresponding to both models is addressed in §3. Finally, main conclusions are presented in §4 and three Appendices contain some mathematical details.

2. Model equations

2.1. *The IL^∞ model*

2.1.1. *Total fields*

Consider an active layer of fluid confined to the uppermost region of the ocean overlying a motionless (infinitely deep) passive layer. Let $-h(\boldsymbol{x}, t) \leqslant z \leqslant 0$ be the

active-layer definition where $\boldsymbol{x}$ is the horizontal position having Cartesian coordinates x and y; z is the upward Cartesian coordinate and t is the time. The equations of motion in the primitive equations model (i.e. with the hydrostatic approximation and the Coriolis force in the horizontal directions) for an active layer with an arbitrary vertical structure and without any forcing or dissipation are

$$\mathrm{IL}^{\infty}\mathrm{PEM}: \begin{cases} \mathrm{D}\vartheta/\mathrm{D}t = 0, \\ \boldsymbol{\nabla}\cdot\boldsymbol{u} + \partial_z w = 0, \\ \mathrm{D}\boldsymbol{u}/\mathrm{D}t + f\hat{\boldsymbol{z}}\times\boldsymbol{u} + \boldsymbol{\nabla}p = 0, \\ \partial_z p - \vartheta = 0, \end{cases} \tag{2.1}$$

where $\mathrm{D}/\mathrm{D}t := \partial_t + \boldsymbol{u}\cdot\boldsymbol{\nabla} + w\partial_z$ is the material derivative; $\boldsymbol{u}(\boldsymbol{x},z,t)$ is the horizontal velocity field with components $u(\boldsymbol{x},z,t)$ and $v(\boldsymbol{x},z,t)$; $w(\boldsymbol{x},z,t)$ is the upward velocity; $\boldsymbol{\nabla}$ is the horizontal gradient operator and $\hat{\boldsymbol{z}}$ is the vertical unit vector. The symbol ϑ denotes the buoyancy and is defined as $\vartheta(\boldsymbol{x},z,t) := -g[\rho(\boldsymbol{x},z,t) - \rho_{deep}]/\rho_0$, where g is the acceleration due to gravity, ρ is the density in the active layer, ρ_{deep} is the constant density in the lower (inactive) layer and ρ_0 is the reference density used in the Boussinesq approximation; p is a kinematic pressure related to the total pressure p_{total} through $p(\boldsymbol{x},z,t) := [p_{total}(\boldsymbol{x},z,t) + \rho_{deep}gz]/\rho_0$ up to the addition of an unimportant constant. The Coriolis parameter f is considered constant throughout the paper. The rigid lid and reduced gravity constraints are imposed through the boundary conditions

$$w = 0 \quad \text{at} \quad z = 0, \tag{2.2}$$

$$p = 0 \quad \text{and} \quad w = -\mathrm{D}h/\mathrm{D}t \quad \text{at} \quad z = -h. \tag{2.3}$$

2.1.2. *Basic state*

As in R95 and R97 the basic flow is chosen as parallel with a linear vertical shear; the Brunt–Väisälä frequency is assumed uniform. The geostrophic balance requires the velocity, buoyancy and layer's depth to be written as (see Appendix A)

$$U(z) = \bar{U} + \left(1 + 2\frac{z}{H_r}\right) U_\sigma, \tag{2.4}$$

$$\Theta(y,z) = g_r\left[1 + \left(1 + 2\frac{z}{H_r}\right) S - 2\frac{fU_\sigma}{g_r H_r} y\right], \tag{2.5}$$

$$H(y) = H_r + \frac{f}{g_r}\left(\frac{U_\sigma - \bar{U}}{1 - S}\right) y \tag{2.6}$$

$+ O(\varepsilon^2)$, where $\varepsilon \to 0$ is a Rossby number and

$$S := \frac{N_r^2 H_r}{2g_r}. \tag{2.7}$$

Notice that, up to $O(\varepsilon)$, the velocity varies from $\bar{U} - U_\sigma$ at the bottom of the layer, to $\bar{U} + U_\sigma$ at the top. Hence, the velocities $\bar{U}$ and U_σ can be taken as those defined in R95 in σ-coordinates.

The parameter S is introduced as a measure of the stratification within the upper layer in a stable stratified reference state without currents. To lowest order in ε (or without currents) the buoyancy is $g_r[1 + (1 + 2z/H_r)S]$, i.e. it varies from $g_r(1 - S)$, at the bottom, to $g_r(1 + S)$, at the top. Consequently, physically acceptable values for S must satisfy

$$0 < S < 1, \tag{2.8}$$

as a condition for the buoyancy to be everywhere positive and the density to increase with depth. Notice that the size of the density gradient is not limited whatsoever: the buoyancy change within the active layer, $N_r^2 H_r = 2Sg_r$, can be made as large as desired while keeping fixed the buoyancy jump at the base $g_r(1-S)$.

Small values of S correspond to weak stratifications, whereas finite values of S imply stronger stratifications. In the limit $S \to 1$ with g_r finite, the buoyancy jump at the interface between the upper layer and the deep ocean vanishes. In this unusual case, the implicit assumption is that $S \to 1$ more slowly than $\varepsilon \to 0$, as required by the hypothesis of very small interface slope in (2.6).

As can be seen in (2.6), a geostrophic current with uniform vertical shear requires a non-horizontal bottom since, in general, there is no need to set $\bar{U} = U_\sigma$, which would correspond to a vanishing value of the velocity at the interface (recall that the lower layer is motionless). In order to focus attention on instability processes related to $\partial_y \Theta$ (instead of $\mathrm{d}H/\mathrm{d}y$), FMP chose $\bar{U} = U_\sigma$. In the present research the effects of $\mathrm{d}H/\mathrm{d}y$ are incorporated and shown to be dynamically important for the baroclinic instability problem.

2.1.3. *Perturbations*

Assume a perturbation with a plane wave structure in x and time so that, for instance, the velocity u is split as

$$u = U(z) + au'(y,z)\mathrm{e}^{\mathrm{i}(kx-\omega t)} + O(a^2), \tag{2.9}$$

where a is an infinitesimal wave amplitude (with the proper units). The $O(a)$ contribution to (2.1) is given by

$$\left.\begin{aligned} \mathrm{i}(kU-\omega)\vartheta' - 2f\frac{U_\sigma}{H_r}v' + N_r^2 w' &= 0, \\ \mathrm{i}ku' + \partial_y v' + \partial_z w' &= 0, \\ \mathrm{i}(kU-\omega)\boldsymbol{u}' + 2\frac{U_\sigma}{H_r}w'\hat{\boldsymbol{x}} + f\hat{\boldsymbol{z}}\times\boldsymbol{u}' + \left(\mathrm{i}k, \partial_y\right)p' &= 0, \\ \partial_z p' - \vartheta' &= 0. \end{aligned}\right\} \tag{2.10}$$

The $O(a)$ boundary conditions (2.2) and (2.3) are

$$w' = 0 \quad \text{at} \quad z = 0, \tag{2.11}$$

$$g_r(1-S)w' + f\left(U_\sigma - \bar{U}\right)v' = -\mathrm{i}\left(kU-\omega\right)p' \quad \text{at} \quad z = -H_r. \tag{2.12}$$

(The derivation of the bottom boundary condition for the linearized problem is straightforward by use of the definition of the kinematic pressure p; it involves a simple expansion in Taylor series about the depth of the layer in the reference state as is shown in Appendix B.) Only the lowest order in ε of the basic fields is considered from (2.10)–(2.12); the order of magnitud of the perturbation fields is treated in §3.1.

Notice that $R_I \equiv (2S)^{1/2} R_E$. Thus in the limit of very weak stratification ($S \to 0$) there is a large separation between the two scales in (1.1), $R_E \gg R_I$, and then long or short perturbations are possible to identify, according to their length scale L:

$$\text{long perturbations} : L \sim R_E \gg R_I$$

or

$$\text{short perturbations} : L \sim R_I \ll R_E.$$

The parameters g_r and N_r, which define the buoyancy profile in the basic state, have been replaced by g_r and S in (2.4)–(2.12). The limit of weak stratification can be

understood in two senses: either $S \to 0$ with g_r fixed or $S \to 0$ with Sg_r ($\propto N_r^2$) fixed. The first (second) case corresponds to the scaling of long (short) perturbations and is formally equivalent to making $N_r \to 0$ ($g_r \to \infty$) while keeping g_r (N_r) finite. The former corresponds to a situation in which the active-layer bottom is free to deform, because (2.12) allows for a finite value of w' at the bottom. The latter corresponds to a case in which the bottom is effectively rigid, since (2.12) requires $w' = 0$ at the bottom. Consequently, the short-perturbation limit corresponds to the well-known Eady problem. FMP studied the long-perturbation limit but concentrated their research on the particular case in which the layer thickness in the basic state is chosen to be constant ($\bar{U} = U_\sigma$). For stronger stratifications (finite S) there is no distinction between long and short perturbations, and the bottom always behaves as a free boundary.

Even though typical values of S are reported quite small (see for instance Tandon & Garrett 1995), it is considered worthwhile to extend the analysis to its whole range of variation (2.8) in order to account for the effects of the increase of the stratification (and, hence, the effects of a free boundary) on the baroclinic instability problem. In the following section it will be shown that the dispersion relations corresponding to long and short perturbations can be seen as limiting cases of a general theory that does not impose any restriction on the size of the stratification parameter S more than that required for static stability (2.8).

2.2. *The IL^1 model*

The model developed in R95 uses the buoyancy field varying linearly with depth, with coefficients that are functions of the horizontal position and time, namely

$$\vartheta(\boldsymbol{x}, \sigma, t) = \bar{\vartheta}(\boldsymbol{x}, t) + \sigma\vartheta_\sigma(\boldsymbol{x}, t),$$

where the overbar indicates vertical average and $\sigma := 1 + 2z/h$ is a scaled vertical coordinate that ranges from $\sigma = -1$ (at the base of the active layer) to $\sigma = 1$ (at the top of the surface). The vertical structure of the velocity field in the IL^{1}PEM is also set linear in σ, i.e. $\boldsymbol{u}(\boldsymbol{x}, \sigma, t) = \bar{\boldsymbol{u}}(\boldsymbol{x}, t) + \sigma\boldsymbol{u}_\sigma(\boldsymbol{x}, t)$, and the equations of motion are obtained by projecting the exact three-dimensional primitive equations system IL$^\infty$PEM into a linear σ-dependence. (Recall that in any primitive equations model, $\boldsymbol{u}$ is independent of ϑ and h.) This model has been shown to have the following concrete properties that contribute to its validity:

(i) Energy, momentum, volume, mass and buoyancy variance are conserved. Furthermore, the densities of these integrals of motion are the same as those of the IL$^\infty$ model.

(ii) The evolution of the vorticity field is correctly represented.

(iii) Linear waves riding on a steady state with no currents are, to a very good approximation, those of the first two vertical modes of the IL$^\infty$ model.

A low-frequency approximation to the IL^{1}PEM, i.e. the IL^{1}QGM, is developed in R97. The horizontal velocity field of R97 is non-divergent and in thermal-wind balance, and therefore the velocity field does not vary just linearly with depth. Instead, the streamfunction is written in the form

$$\psi(\boldsymbol{x}, \sigma, t) = \bar{\psi}(\boldsymbol{x}, t) + \sigma\psi_\sigma(\boldsymbol{x}, t) + \tfrac{1}{2}\left(\sigma^2 - \tfrac{1}{3}\right)\psi_{\sigma\sigma}(\boldsymbol{x}, t),$$

where

$$\begin{pmatrix} \bar{\psi} \\ \psi_\sigma \\ \psi_{\sigma\sigma} \end{pmatrix} = \begin{pmatrix} 1 - S/3 & 1/2 & -S/6 \\ S/2 & 1/2 & 0 \\ -S/2 & 0 & S/2 \end{pmatrix} \begin{pmatrix} \varphi_1 \\ \varphi_2 \\ \varphi_3 \end{pmatrix} \tag{2.13}$$

with

$$\varphi_1 := fR_E^2\left(\frac{h}{H_r}-1\right), \quad \varphi_2 := fR_E^2\left(\frac{\bar{\vartheta}}{g_r}-1\right), \quad \varphi_3 := fR_E^2\left(\frac{\vartheta_\sigma}{Sg_r}-1\right), \tag{2.14}$$

and it is assumed that $\varphi_j \ll fR_E^2$. (The determinant of the transformation matrix in (2.13) vanishes for $S = 0$ and $S = 1$, and therefore the transformation is invertible since these values lie outside the physical range $0 < S < 1$, which also holds for the present approximate model.) The evolution equations are

$$\mathrm{IL}^1\mathrm{QGM}: \begin{cases} \partial_t\bar{\xi} + \left[\bar{\psi},\bar{\xi}\right] + \frac{1}{3}\left[\psi_\sigma,\xi_\sigma\right] + \frac{1}{6}SR_E^{-2}\left[\varphi_1,\varphi_3\right] = 0, \\ \partial_t\xi_\sigma + \left[\bar{\psi},\xi_\sigma\right] + \left[\psi_\sigma,\bar{\xi}\right] + R_E^{-2}\left[\varphi_1+\varphi_3, S\varphi_1+\frac{1}{2}\varphi_2\right] = 0, \\ \partial_t\varphi_3 + \left[\bar{\psi},\varphi_3\right] + \frac{1}{2}\left[\varphi_1,\varphi_2\right] = 0, \end{cases} \tag{2.15}$$

where $[A,B] := \hat{\boldsymbol{z}}\cdot\nabla A\times\nabla B$ is the horizontal Jacobian of the functions A and B, and

$$\bar{\xi} := f + \nabla^2\bar{\psi} - R_E^{-2}\varphi_1, \quad \xi_\sigma := \nabla^2\psi_\sigma - 6R_I^{-2}\varphi_2 \tag{2.16}$$

(see R97 for details).

3. Normal-modes stability analysis

In the present section general low-frequency analytic expressions for the normal modes and their dispersion relation are derived, restricted to neither a weak stratification nor a constant layer thickness in the basic state. This is done for both models IL^∞ and IL^1. The long- and short-perturbations cases are obtained as the limits of weak stratification ($S \to 0$), with $L \sim R_E$ and $L \sim R_I$ respectively, of the general dispersion relation corresponding to each model. The IL^1 model is shown to give the exact expression for the dispersion relation of long perturbations. Its behaviour at strong stratifications is found not to follow exactly that of the IL^∞ model.

3.1. *Results for the IL$^\infty$ model*

In order to quantify the restrictions built into the analytic solution, the following scalings are proposed:

$$(\boldsymbol{x},z,t) \sim \left(L,H_r,\frac{1}{\varepsilon f}\right), \quad (\boldsymbol{u}',w') \sim \left(\varepsilon Lf,\varepsilon^2H_rf\right), \quad \left(h',\vartheta',p'\right) \sim \left(\varepsilon H_r,\varepsilon\frac{L^2f^2}{H_r},\varepsilon L^2f^2\right).$$

Recall, from Appendix A, that $\bar{U}, U_\sigma \sim \varepsilon Lf$ where $\varepsilon \to 0$. The election of $1/(\varepsilon f)$ as the characteristic time scale restricts the analysis to low-frequency waves. The low-frequency nature of the dynamics requires a vanishing $O(\varepsilon)$ contribution to w'. In consequence, an extra factor of ε is included in the scale of w'. All these assumptions are nothing but the standard ones made in classical quasi-geostrophic theory (Pedlosky 1987).

A correct way to achieve the weak stratification–small Rossby number limit is to define a positive constant v such that

$$S = O\left(\varepsilon^v\right) \text{ as } \varepsilon \to 0.$$

The Richardson number is $Ri := \left(N_r/\partial_z U\right)^2 \equiv \frac{1}{4}N_r^2H_r^2/U_\sigma^2 \sim \varepsilon^{-2}R_I^2/L^2$; consequently $Ri = O(\varepsilon^{-2})$ in the general case, finite S, as well as in the short perturbations case of the $S \to 0$ limit. This implies $Ri \to \infty$ as $\varepsilon \to 0$, which is a well-known assumption for the Eady problem. However, in the long-perturbations case $Ri \sim \varepsilon^{-2}S = O(\varepsilon^{v-2})$ and

therefore Ri might also remain finite ($v = 2$) or even tend to zero ($v > 2$) as $\varepsilon \to 0$. This is an important extension of the baroclinic instability problem, since Tandon & Garrett (1995) argue that the restratification process leads to $Ri \approx 1$.

According to the scalings introduced above it follows that the relative orders of magnitude among the various terms of the linearized equations (2.10) are

$$\left.\begin{aligned} \underset{\varepsilon^2}{\mathrm{i}(kU-\omega)}\,\vartheta' - 2f\underset{\varepsilon^2}{U_\sigma H_r^{-1}}v' + \underset{\varepsilon^2 R_I^2/L^2}{N_r^2 w'} &= 0,\\ \underset{\varepsilon}{\mathrm{i}k u'} + \underset{\varepsilon}{\partial_y v'} + \underset{\varepsilon^2}{\partial_z w'} &= 0,\\ \underset{\varepsilon^2}{\mathrm{i}(kU-\omega)}\,\boldsymbol{u}' + \underset{\varepsilon^3}{2U_\sigma H_r^{-1} w'\hat{\boldsymbol{x}}} + f\hat{\boldsymbol{z}}\times\boldsymbol{u}' + \underset{\varepsilon}{\left(\mathrm{i}k, \partial_y\right)} p' &= 0,\\ \underset{\varepsilon}{\partial_z p'} - \underset{\varepsilon}{\vartheta'} &= 0. \end{aligned}\right\} \tag{3.1}$$

Whereas, for the bottom boundary condition (2.12) it follows that

$$\underset{\varepsilon^2 R_E^2/L^2}{g_r(1-S)}\,w' + f\underset{\varepsilon^2}{\left(U_\sigma - \bar{U}\right)}v' = -\underset{\varepsilon^2}{\mathrm{i}(kU-\omega)}\,p' \quad \text{at} \quad z = -H_r. \tag{3.2}$$

Let now expand all perturbation fields as well as the phase speed as regular asymptotic expansions of the form

$$\begin{array}{rcccccc} \boldsymbol{u}' & = & \mathrm{i}(-l,k)\,\psi' \mathrm{e}^{\mathrm{i}ly} & + & \boldsymbol{u}_2' & + & \ldots,\\ w' & = & & & \mathrm{i}k\varpi \mathrm{e}^{\mathrm{i}ly} & + & \ldots,\\ p' & = & f\psi' \mathrm{e}^{\mathrm{i}ly} & + & p_2' & + & \ldots,\\ \vartheta' & = & f(\mathrm{d}\psi'/\mathrm{d}z)\mathrm{e}^{\mathrm{i}ly} & + & \vartheta_2' & + & \ldots,\\ \omega & = & kc & + & \omega_2 & + & \ldots.\\ O & : & \varepsilon & & \varepsilon^2 & & \varepsilon^3 \end{array}$$

The perturbation streamfunction $\psi'(z)$ is introduced since the $O(\varepsilon)$ horizontal velocity is non-divergent. The function $\varpi(z)$ is proportional to the amplitude of the lowest-order perturbation vertical velocity, while the accompanying factor $\mathrm{i}k$ is introduced for convenience. Notice that a wave-like structure in the y-coordinate is assumed at lowest order since at this level no y-dependent terms appear in the equations of motion or the bottom boundary condition. Because the basic physics of the instability appears at lowest order, there will be no need to seek higher order solutions than that corresponding to the eigenvalue c, which is $O(\varepsilon)$. To achieve this, however, it is necessary to deal with $O(\varepsilon^2)$ dynamics, which is governed by the lowest order contribution to the buoyancy conservation equation (3.1, first equation), i.e.

$$(U-c)\frac{\mathrm{d}\psi'}{\mathrm{d}z} - 2\frac{U_\sigma}{H_r}\psi' + \frac{N_r^2}{f}\varpi = 0, \tag{3.3}$$

and by the vorticity equation

$$(U-c)\boldsymbol{k}^2\psi' + f\frac{\mathrm{d}\varpi}{\mathrm{d}z} = 0, \tag{3.4}$$

which follows after taking the curl of the $O(\varepsilon^2)$ horizontal momentum equations and combining the result with the $O(\varepsilon^2)$ volume conservation law. Equations (3.3) and

(3.4) are subject to the boundary conditions

$$\varpi(0) = 0 \quad \text{and} \quad \varpi(-H_r) = \frac{fc}{g_r(1-S)}\psi'(-H_r), \tag{3.5}$$

which follow from (2.2) and (3.2). If the second-order field ϖ is eliminated between (3.3) and (3.4), a single equation for the first-order perturbation streamfunction field follows, i.e.

$$(U-c)\left[\frac{\mathrm{d}^2\psi'}{\mathrm{d}z^2} - \frac{\kappa_I^2}{H_r^2}\psi'\right] = 0, \tag{3.6}$$

with $\kappa_I^2 := \boldsymbol{k}^2 R_I^2$, which is the well-known quasi-geostrophic potential vorticity equation. Finally, to close the problem it is necessary to rewrite the boundary conditions (3.5) in terms of the perturbation streamfunction. This is achieved by use of (3.3) and the result is

$$(U-c)\,H_r\frac{\mathrm{d}\psi'}{\mathrm{d}z} = 2U_\sigma\psi' \quad \text{at} \quad z = 0, \tag{3.7}$$

$$(U-c)\,H_r\frac{\mathrm{d}\psi'}{\mathrm{d}z} = 2\left(U_\sigma - \frac{Sc}{1-S}\right)\psi' \quad \text{at} \quad z = -H_r. \tag{3.8}$$

Consider first the non-singular solutions of (3.6), i.e. solutions such that the bracketed quantity in (3.6) vanishes. A solution that satisfies the surface boundary condition (3.7) is found to be

$$\psi'(z) = \left(c - \bar{U} - U_\sigma\right)\kappa_I \cosh\kappa_I\frac{z}{H_r} - 2U_\sigma \sinh\kappa_I\frac{z}{H_r}. \tag{3.9}$$

The bottom boundary condition (3.8) then yields a second-order algebraic equation in c whose solutions give the dispersion relation

$$c = \bar{U} + \frac{S\left[\left(U_\sigma - \bar{U}\right) - 2U_\sigma\kappa_I^{-1}\tanh\kappa_I\right] \pm U_\sigma\Delta^{1/2}}{2S + (1-S)\,\kappa_I\tanh\kappa_I} \tag{3.10}$$

where

$$\begin{aligned}\Delta = {} & \left\{4S^2\kappa_I^{-2} + 4(S-1)\left[\left(1+\bar{U}/U_\sigma\right)S - 1\right] + (S-1)^2\kappa_I^2\right\}\tanh^2\kappa_I \\ & + \left[2 - \left(3 + \bar{U}/U_\sigma\right)S\right]\left[4S\kappa_I^{-1} + 2(S-1)\,\kappa_I\right]\tanh\kappa_I \\ & + S^2\left[9 + \bar{U}/U_\sigma\left(2 + \bar{U}/U_\sigma\right)\right] - 8S.\end{aligned}$$

Dispersion relation (3.10) will be referred to as the general one, because those corresponding to the long- and short-perturbation limits can be derived from this one.

For each real horizontal wavenumber, the normal-mode analysis yields two modes in z with eigenvalue c given by (3.10). These two modes are far from spanning a complete basis that can be use to represent a perturbation with arbitrary vertical structure. In order to complete the basis, it is necessary to account also for the singular solutions of (3.6), i.e. those solutions satisfied for real c such that

$$\frac{\mathrm{d}^2\psi'}{\mathrm{d}z^2} - \frac{\kappa_I^2}{H_r^2}\psi' = b\delta(z - z_c),$$

where $c = U(z_c)$, $\delta(\cdot)$ is the Dirac delta function and $b(\kappa_I^2, z_c/H_r)$ is, in general, a non-zero constant. There are an infinite number of solutions exponentially trapped to a critical level z_c (see for instance Pedlosky 1987), each corresponding to a real value

of c in the continuous range

$$\left|c-\bar{U}\right|<\left|U_{\sigma}\right|. \tag{3.11}$$

Notice that this continuous spectrum of eigenvalues, required for completeness of the total solution, corresponds only to neutrally stable perturbations. Thus there will be no need to further discuss the continuous spectrum as far as the instability problem is concerned, and the non-singular solutions of (3.6) will be sufficient for the purpose of the present research. However, it should be mentioned that although the long-time asymptotic behaviour is dominated by the discrete exponentially growing normal modes, initial intensification can be shown to be dependent on the continuous spectrum (e.g. see Farrell 1982).

3.1.1. *Weak stratification*

This limit corresponds to $S\to 0$ and two cases are of interest, according to whether $L\sim R_E$ or $L\sim R_I$. In the first case, the last term in (3.1, first equation), vertical advection of ambient buoyancy, can be neglected, since $R_I^2/L^2\sim S$. In the second case, the first term in (3.2) is the dominant one, since $R_E^2/L^2\sim S^{-1}$.

(*a*) *Long perturbations:* $L\sim R_E\gg R_I$

The density (3.3) and vorticity (3.4) equations reduce to

$$(U-c)\frac{\mathrm{d}\psi'}{\mathrm{d}z}-2\frac{U_{\sigma}}{H_r}\psi'=0,\quad (U-c)\boldsymbol{k}^2\psi'+f\frac{\mathrm{d}\varpi}{\mathrm{d}z}=0, \tag{3.12}$$

with boundary conditions

$$\varpi(0)=0\quad\text{and}\quad\varpi(-H_r)=\frac{fc}{g_r}\psi'(-H_r), \tag{3.13}$$

Non-trivial solutions are given by

$$\psi'(z)=U-c \tag{3.14}$$

and

$$\varpi(z)=-\frac{\boldsymbol{k}^2H_r}{6fU_{\sigma}}\left[(U-c)^3-\left(\bar{U}+U_{\sigma}-c\right)^3\right], \tag{3.15}$$

where the eigenvalue c satisfies the following dispersion relation:

$$\text{long perturbations:}\quad\begin{cases} c=\dfrac{\left(1+2\kappa_E^2\right)\bar{U}-U_{\sigma}\pm\Delta^{1/2}}{2+2\kappa_E^2}, \\ \Delta=\left(\bar{U}-U_{\sigma}\right)^2-4\kappa_E^2U_{\sigma}\left[\bar{U}+\frac{1}{3}\left(1+\kappa_E^2\right)U_{\sigma}\right], \end{cases} \tag{3.16}$$

with $\kappa_E^2:=\boldsymbol{k}^2R_E^2$. Notice that the above dispersion relation can also be obtained from the general one (3.10) on making the replacement $\kappa_I=(2S)^{1/2}\kappa_E$ and taking the limit $S\to 0$ at fixed κ_E, as long as

$$\bar{U}/U_{\sigma}\ll O\left(S^{-1}\right). \tag{3.17}$$

In addition, the streamfunction (3.14) is also found to be the lowest-order contribution in S to (3.9). Analysis of the instability for very weak shears (or, equivalently, slopes of the interface of the same order as that of isopycnals) e.g. $\bar{U}/U_{\sigma}=O\left(S^{-1}\right)$ as $S\to 0$, goes beyond the scope of the present paper but is presented in (Ripa 1997*b*).

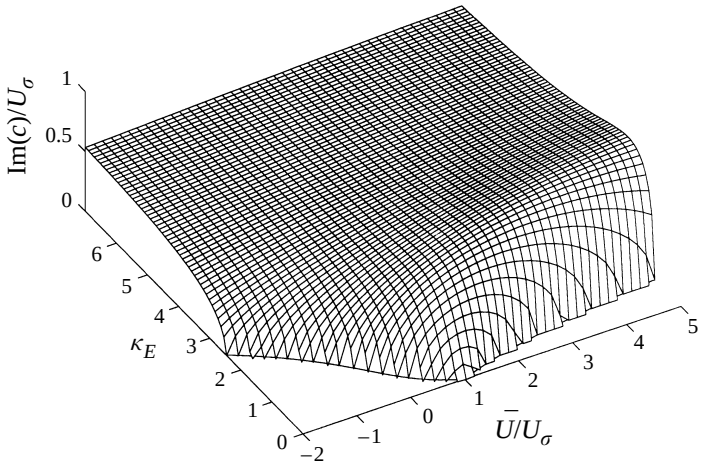

FIGURE 1. Imaginary part of the eigenvalue c for (growing) long perturbations in the exact IL$^{\infty}$ model as a function of the non-dimensional perturbation horizontal wavenumber $\kappa_E := |\boldsymbol{k}|\, R_E$ and the ratio $\bar{U}/U_\sigma$, where R_E is the deformation radius in the first ('external') vertical normal mode when the stratification is very weak, and the basic current at the active-layer surface and bottom equals $\bar{U} + U_\sigma$ and $\bar{U} - U_\sigma$. Notice that there is always a range of stable wavenumbers except for $\bar{U}/U_\sigma = 1$ and that the asymetry between $\bar{U}/U_\sigma > 1$ and $\bar{U}/U_\sigma < 1$. There is no difference between this result and those corresponding to the approximate models IL^1 (Ripa 1995, 1997*a*) and the $\mu \to 0$ limit of the SML (Young & Chen 1995).

A condition for the existence of growing and decaying normal modes, $\mathrm{Im}(c) \neq 0$, is that $\Delta < 0$. Hence, all horizontal perturbation wavenumbers such that

$$\kappa_E^2 > \kappa_{E_{crit.}}^2 = \left[1 + 3\left(\bar{U}/U_\sigma\right)^2\right]^{1/2} - \tfrac{1}{2}\left(1 + 3\bar{U}/U_\sigma\right) \tag{3.18}$$

are found to be unstable with a vanishing critical wavenumber for $\bar{U}/U_\sigma = 1$. Equations (3.16) and (3.18) were first discussed in R95 and R97, where β-effects are also considered.

Stone (1966) found the $\kappa_E \to \infty$ limit of the relation (3.16), i.e. the situation in which the active-layer bottom is not free to deform, and included ageostrophic corrections. FMP, using a free bottom condition, worked with the $\bar{U}/U_\sigma = 1$ case and concluded that all wavenumbers were unstable ($\kappa_{E_{crit.}} = 0$), i.e. there is no long-wave cutoff (it makes no sense to talk of a short-wave cutoff in a long-wave theory.) The most striking difference between relation (3.16) and that of FMP is that for $\bar{U}/U_\sigma \neq 1$ (i.e. a non-horizontal layer bottom in the basic state) the flow is more stable to long perturbations, in the sense that there is a finite long-wave cutoff. This is evident when the imaginary part of the eigenvalue c, corresponding to the growing mode, is plotted as a function of the perturbation horizontal wavenumber and the ratio $\bar{U}/U_\sigma$, as is done in figure 1. Notice that the flow appears to be more stable when $\bar{U}/U_\sigma < 1$ than when $\bar{U}/U_\sigma > 1$. The case $\bar{U}/U_\sigma < 1$ (> 1) corresponds to a situation in which the depth and the buoyancy in the basic state increase along the y-direction in the same (opposite) sense. In figure 2 the dispersion relation (3.16) is plotted as a function of the perturbation horizontal wavenumber for various values of $\bar{U}/U_\sigma$ where it is clear that the onset of the instability at $\kappa_{E_{crit.}}$ is a result of the collision of the c_+ and c_- branches of (3.16). (For the case $\bar{U}/U_\sigma = 1$ the collision occurs at $\kappa_{E_{crit.}} = 0$ and hence all long wavelengths are unstable.)

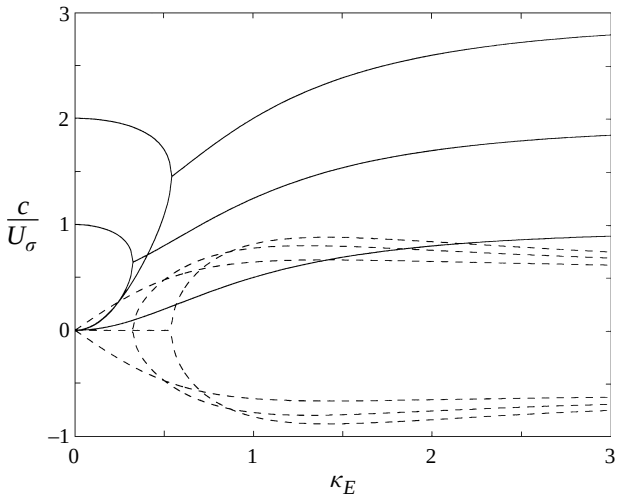

FIGURE 2. Dispersion curves for the real and the imaginary parts of the eigenvalue c for long perturbations as a function of the horizontal wavenumber in the IL^∞ model. The real part of c is the solid curve whereas the imaginary part (indicating instability) is dashed. The instability starts at the wavenumber where the c_+ and c_- branches collide. The three cases correspond to $\bar{U}/U_\sigma = 1$, 2 and 3, ordered by the bifurcation point. In particular, for the case $\bar{U}/U_\sigma = 1$, the collision occurs at $\kappa_E = 0$ and hence the perturbation has a non-vanishing growth rate at all (long) wavenumbers. The curves corresponding to the approximate models IL^1 and SML collapse into these exact ones, in the limit of weak stratification ($S \to 0$).

As far as the vertical structure of the lowest order perturbation fields is concerned, it follows from (3.14) that the horizontal velocity and pressure are linear functions of depth, the buoyancy perturbation is uniform whilst the vertical velocity is cubic (instead of exponential, as it is in the case of strong stratifications or the short-perturbation limit). Notice that the eigenproblem (3.12)–(3.13) also has an infinite number of singular eigensolutions in the continuous spectrum of real eigenvalues (3.11).

(*b*) *Short perturbations*: $L \sim R_I \ll R_E$

In this limit the eigenproblem (3.6)–(3.8) reduces to that of the well-known Eady model whose non-singular eigensolutions are (3.9) with eigenvalues given by

$$\text{Eady}: \; c = \bar{U} \pm U_\sigma \left[\left(1 - 2\kappa_I^{-1} \tanh \tfrac{1}{2}\kappa_I\right)\left(1 - 2\kappa_I^{-1} \coth \tfrac{1}{2}\kappa_I\right)\right]^{1/2} \tag{3.19}$$

(e.g. see Gill 1982 or Pedlosky 1987). It is worth mentioning that the general dispersion relation (3.10) contains Eady's, as the limit $S \to 0$ with κ_I fixed, subject to the restriction (3.17); see (Ripa 1997*b*) for an extension beyond it. The singular eigensolutions in this limit are similar in character to those corresponding to strong stratifications since both sets of eigensolutions follow from the potential vorticity equation (3.6).

Notice that the limit of (3.19) when $\kappa_I \to 0$ coincides with that of (3.16) when $\kappa_E \to \infty$, i.e. $c = \bar{U} \pm \mathrm{i}U_\sigma\sqrt{1/3}$, as is expected for a correct matching between both asymptotic solutions. A very important property of (3.19) is the existence of a high-wavenumber cutoff of the instability, namely c is real for $\kappa_I > \kappa_{I_{crit.}} \approx 2.4$. (A physical explanation of the existence of such a high-wavenumber cutoff can be found in Pedlosky (1987).) This result is independent of the magnitude of the ratio

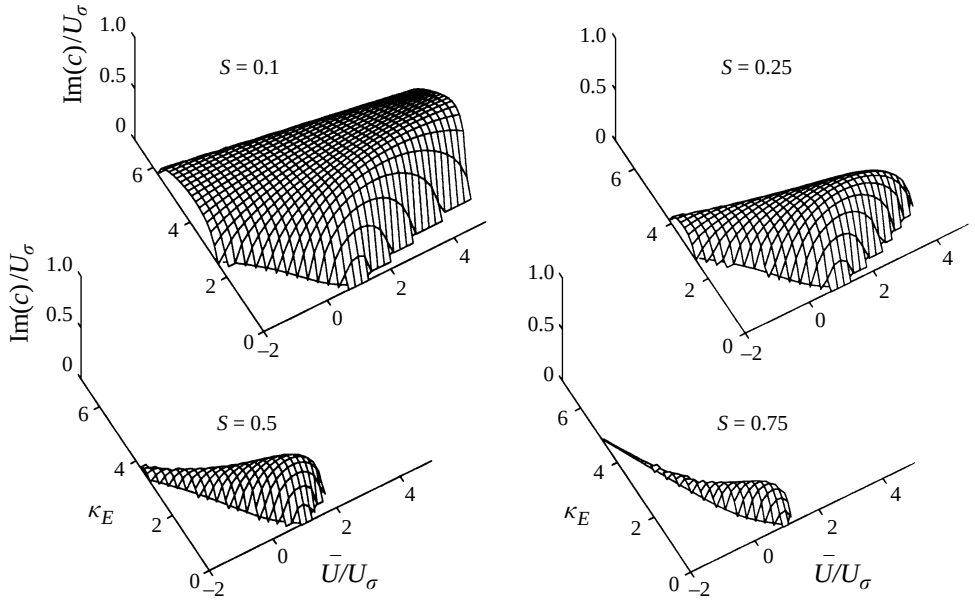

FIGURE 3. Imaginary part of the eigenvalue c for the growing mode in the IL$^\infty$ model as a function of the perturbation horizontal wavenumber and the ratio $\bar{U}/U_\sigma$ for different finite values of the stratification parameter $S := \frac{1}{2}N_r^2 H_r/g_r$ where N_r^2, g_r and H_r are the Brunt–Väisälä frequency squared, the mean buoyancy and the depth of the layer in a reference state without currents. Notice that the growth rate of the perturbation goes to zero when S approaches unity.

$\bar{U}/U_\sigma$, i.e. whether the base of the active layer in the basic state is sloped or not is immaterial, except for the restriction (3.17). The independence of $\bar{U}/U_\sigma$ comes from the fact that over one horizontal length L, the relative elevation of the interface is $O(\varepsilon L^2/R_E^2)$; see (2.6). In the quasi-geostrophic scaling, the relevant non-dimensional measure of the slope is thus L^2/R_E^2, which goes to zero for short perturbations. FMP obtained only the $\kappa_I \to 0$ limit of Eady's dispersion relation, and for $\bar{U}/U_\sigma = 1$, namely $c = U_\sigma(1 \pm \mathrm{i}\sqrt{1/3})$.

3.1.2. *Strong stratification*

The range of interest in the parameter space is now $0 < S < 1$. The imaginary part of the general dispersion relation (3.10) corresponding to the growing mode is displayed in figure 3 as a function of the perturbation horizontal wavenumber and the ratio $\bar{U}/U_\sigma$, for different values of the stratification parameter S. Notice also the presence of a short-wave cutoff of the instability, which is found for all value of $\bar{U}/U_\sigma$ and S. In figure 3 it is also evident that the increase in stratification inhibits the ability of the perturbation to grow. Moreover, in the limit $S \to 1$ it follows that the dispersion relation (3.10) reduces to

$$c_+ = \bar{U} + U_\sigma - 2U_\sigma \kappa_I^{-1} \tanh \kappa_I \quad \text{and} \quad c_- = 0, \tag{3.20}$$

i.e. the growth rate of the perturbation vanishes at all wavenumbers for any choice of $\bar{U}/U_\sigma$.

3.2. *Results for the IL^1 model*

The stability to normal-mode perturbations of a basic state equivalent to that used for the IL$^\infty$ model is studied assuming

$$\varphi_j = -A_j y + a\varphi'_j \mathrm{e}^{\mathrm{i}[k(x-ct)+ly]} + O(a^2)$$

and replacing in the model equations (2.15), which gives

$$\left.\begin{aligned}
&\left(\bar{U}-c\right)\bar{\xi}' + R_E^{-2}A_1\bar{\psi}' + \tfrac{1}{3}U_\sigma\xi'_\sigma + 2R_I^{-2}A_2\psi'_\sigma + \tfrac{1}{6}SR_E^{-2}\left(A_1\varphi'_3 - A_3\varphi'_1\right) = 0,\\
&\left(\bar{U}-c\right)\xi'_\sigma + 6R_I^{-2}A_2\bar{\psi}' + U_\sigma\bar{\xi}' + R_E^{-2}A_1\psi'_\sigma\\
&\qquad + R_E^{-2}\left[\left(A_1+A_2\right)\left(S\varphi'_1 + \tfrac{1}{2}\varphi'_2\right) - \left(SA_1 + \tfrac{1}{2}A_2\right)\left(\varphi'_1 + \varphi'_3\right)\right] = 0,\\
&\left(\bar{U}-c\right)\varphi'_3 A_3\bar{\psi}' + \tfrac{1}{2}\left(A_1\varphi'_2 - A_2\varphi'_1\right) = 0,
\end{aligned}\right\} \tag{3.21}$$

where

$$\begin{pmatrix} A_1 \\ A_2 \\ A_3 \end{pmatrix} = (S-1)^{-1}\begin{pmatrix} -1 & 1 \\ S & S-2 \\ -1 & 1 \end{pmatrix}\begin{pmatrix} \bar{U} \\ U_\sigma \end{pmatrix}. \tag{3.22}$$

In R95 the eigensolutions of the system (3.21), including β-effects, are studied in the limit $S \to 0$. In order to make a comparison with the results from the exact IL$^\infty$ model of the previous section, S will be allowed to take finite values. The problem for the eigenvalue c then results in a third-order algebraic equation as is shown in Appendix C.

3.2.1. *Weak stratification*

Dispersion relations for the long- and short-perturbation limits were derived in R95 and R97 assuming $S \to 0$ from the beginning of the analysis. In the present formalism they are found as the long- or short-wave limits of relation (C 1) by keeping κ_E fixed or making the replacement $\kappa_E = \kappa_I/(2S)^{1/2}$ with fixed κ_I respectively, and taking the limit $S \to 0$. The corresponding dispersion relations are

$$\text{long perturbations:}\quad \left\{\begin{aligned} c &= \frac{\left(1+2\kappa_E^2\right)\bar{U} - U_\sigma \pm \Delta^{1/2}}{2+2\kappa_E^2},\\ \Delta &= \left(\bar{U}-U_\sigma\right)^2 - 4\kappa_E^2 U_\sigma\left[\bar{U} + \tfrac{1}{3}\left(1+\kappa_E^2\right)U_\sigma\right] \end{aligned}\right. \tag{3.23}$$

and

$$\text{short perturbations:}\ c = \bar{U} \pm U_\sigma\frac{\left[\left(\kappa_I^4 - 144\right)/3\right]^{1/2}}{\kappa_I^2 + 12}, \tag{3.24}$$

with a common third root given by $c = \bar{U}$ ($\psi'_{\sigma\sigma} \neq 0$), which is the mean value of the continuous spectrum of eigenvalues (3.11) required for completeness of the total solution in the IL$^\infty$ model. The absence of a continuous spectrum in the IL^1 model is in agreement with the limited vertical variation for the perturbations allowed by the model.

It is remarkable to notice that the long-perturbation limit (3.23) coincides identically with the exact calculation (3.16) and thus all the results concerning long perturbations alluded to in the previous section also apply to (3.23). The vertical structure of the horizontal velocity and pressure perturbations is linear, whereas the buoyancy is uniform with depth. (The latter is readily seen when taking the limit $S \to 0$ in (2.14, last equation).) Notice that such a vertical structure is exactly the same as that

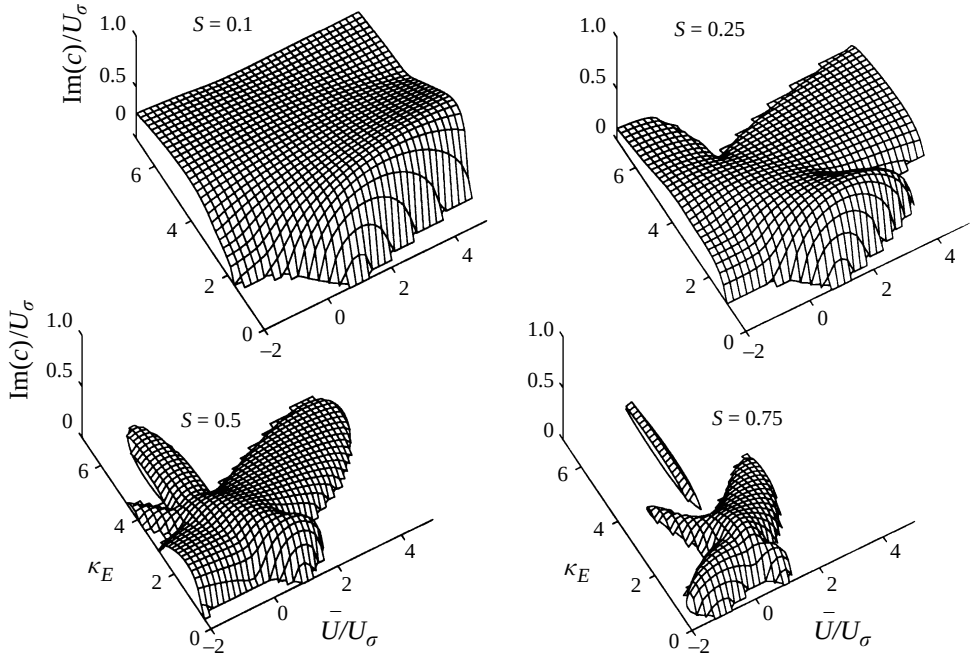

FIGURE 4. As in figure 3 but now for the restricted model IL[1]. Notice that in the limit $S \to 0$ the behaviour of the growth rate of the perturbations is exact (compare with figure 3).

predicted by the IL$^\infty$. The first difference between the two models is found in the structure of the vertical velocity, cubic *vs.* quadratic in z, which is $O(\varepsilon^2)$.

On the other hand, the short-perturbation limit (3.24) is exact as $\kappa_I \to 0$ and has a high-wavenumber cutoff corresponding to $\kappa_{I_{crit.}} = \sqrt{12} \approx 3.46$, which is about 44% larger than that predicted by the Eady model. In addition, the asymptotic value of $c - \bar{U}$ as $\kappa_I \to \infty$ is about 43% smaller. The dispersion relation (3.24), compared to that of Eady, is shown in figure 11 of R95.

3.2.2. *Strong stratification*

In figure 4 the imaginary part of the roots of the polynomial (C 1) are plotted as a function of the perturbation horizontal wavenumber and the ratio $\bar{U}/U_\sigma$, for different values of the stratification parameter S. Notice that the growth rates of the perturbations in the IL[1] model approach those in the IL$^\infty$ model for weak enough stratifications (see figure 3). Only the growth rate of long enough perturbations superimposed on basic states with nearly horizontal lower boundaries behaves similarly to that of the exact model when the stratification is increased, as can be seen in figure 5. The stabilizing tendency on the basic flow as the stratification reaches its maximum is also found in the approximate model, though in the limit $S \to 1$ it follows from (C 1) that

$$c_+ = \bar{U} + \left(\frac{6 + \kappa_I^2}{3 + \kappa_I^2}\right)\frac{U_\sigma}{2} \quad \text{and} \quad c_- = \frac{8\bar{U}}{2 + \kappa_I^2}, \tag{3.25}$$

rather than (3.20). The differences between (3.20) and (3.25) are attributed, as in the short-perturbation limit, to the constraint on the buoyancy to a linear profile in depth, which cannot reproduce the exponential trapping of the exact eigensolutions (3.9).

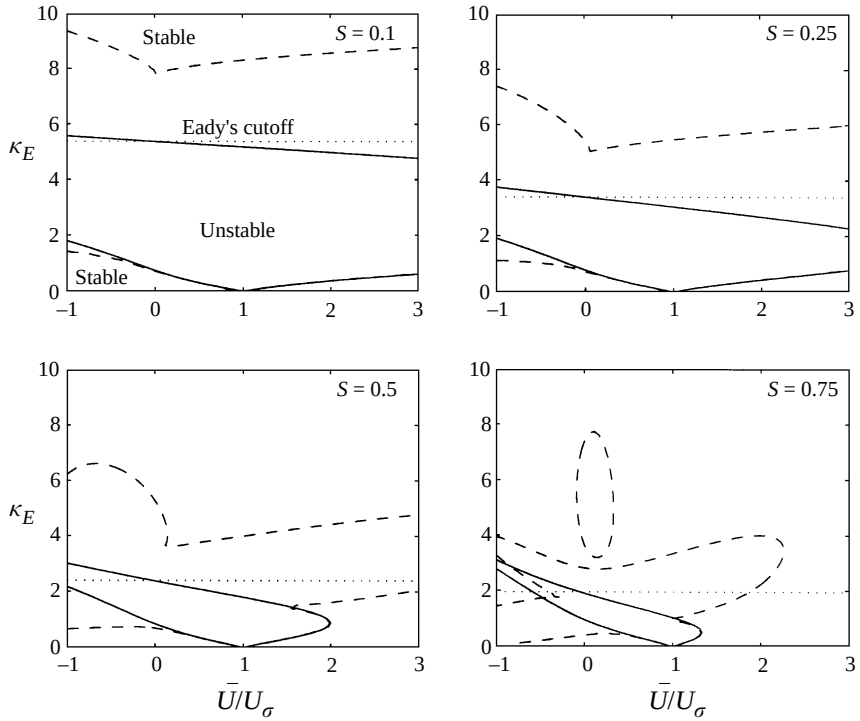

FIGURE 5. Neutral stability curves in the $(\kappa_E, \bar{U}/U_\sigma)$-plane for the IL^∞ (solid) and for the IL^1 (dashed) models for different finite values of the stratification. The dotted line indicates the short-perturbation cutoff in the Eady model, i.e. $\kappa_I := |\boldsymbol{k}| R_I \approx 2.4$, where R_I/π is the deformation radius in the first internal vertical normal mode when the stratification is very weak. Notice that for very strong stratifications (large S) the approximate IL^1 model gives the correct result only near $\kappa_E = 0$ and $\bar{U}/U_\sigma = 1$.

4. Discussion

An analytic expression has been derived for the normal modes superimposed on a basic steady state with uniform density stratification and a parallel current with a uniform vertical shear in thermal-wind balance with the horizontal buoyancy gradient. The basic velocity varies from $\bar{U} + U_\sigma$, at the top, to $\bar{U} - U_\sigma$, at the bottom of the layer. The model, denoted by IL^∞, is a reduced-gravity one on the f-plane, and allows an arbitrary vertical variation for the perturbation fields. The dispersion relation and normal modes structure derived here are valid to lowest order in the Rossby number ε. Neither a weak stratification within the active layer (measured by the parameter S), nor a constant active layer thickness ($\bar{U}/U_\sigma = 1$) in the basic state are imposed as rectrictions.

Two horizontal scales have been introduced, namely R_E and R_I from (1.1). In the limit of very weak stratification ($S \to 0$), in which case the deformation radii of the 'equivalent barotropic' or external mode and the gravest internal mode are R_E and R_I/π respectively, there is a large separation between both scales ($R_E \gg R_I$). Hence, long ($L \sim R_E$) or short ($L \sim R_I$) perturbations can be identified. The associated dispersion relations are found as the long- and short-wave limits of the general one.

(*a*) The short-perturbation limit corresponds to the well-known Eady problem for which the shape of the active-layer bottom in the basic state, e.g. whether it is

horizontal or not, is immaterial. This comes from the fact that in the quasi-geostrophic scaling the relevant non-dimensional mesasure of the slope of the interface, L^2/R_E^2, tends to zero for short perturbations. Moreover, the layer bottom is effectively rigid in this limit. The comparison with the eigenvalues of the approximate model IL^1 (Ripa 1995; Ripa 1997*a*) (which only allows the buoyancy field to vary linearly with depth) shows differences of the order of 40%, though it does have a high-wavenumber cutoff. The reason for the disparities in the results at short wavelengths between the IL^∞ and IL^1 models are attributed to the inefficient representation of the exponential trapping of the Eady problem eigensolutions due to the restriction for the buoyancy to have a linear profile in depth in the IL^1 model.

(*b*) In the long-perturbation limit the bottom is free to deform. The derived dispersion relation is found not to be restricted to any value of the Richardson number, i.e unstable wave solutions are found for $Ri = O(\varepsilon^{\nu-2})$ with $S = O(\varepsilon^\nu)$ for any $\nu > 0$ (in contrast to the short-perturbation limit and the strong stratification case, for which instabilities are found for $Ri = O(\varepsilon^{-2})$). In this limit the stability of the flow is sensible to variations of the layer depth in the basic state. The flow is more stable when $\bar{U}/U_\sigma < 1$ than when $\bar{U}/U_\sigma > 1$. In the first case, the depth and the buoyancy in the basic state increase along the y-direction in the same sense; the second situation corresponds to one in which the y-growth is in the opposite sense. The situation studied by Fukamachi *et al.* (1995), $\bar{U}/U_\sigma = 1$, is recognized as that of maximal instability and it is shown that there is no need to assume any specific value of Ri for its derivation. The vertical structure of the perturbation fields is found to be linear for the horizontal velocity and pressure fields and uniform for the buoyancy. All these results are exactly predicted by the approximate model IL^1 and thus they are an encouraging sign of its validity (at least in the present limit). Moreover, the dispersion relation corresponding to the limit $\mu \to 0$ (see the Introduction) of the SML approximation (Young & Chen 1995) also coincides with the exact one derived here. However, in the SML the buoyancy is uniform in depth but the model has only an implicit representation of the velocity's vertical shear through the thermal-wind balance.

When the stratification is not weak (finite S), the base of the active layer behaves always as a free boundary. Moreover, an increase in stratification is found to contribute to the stabilization of the basic flow. This result is no longer well-represented by the IL^1 model, also as a consequence of its limited vertical structure which does not reproduce the exponential trapping of the IL^∞ model's eigensolutions that appear at stronger stratifications. Nonetheless, it can be said that the growth rate of long enough perturbations superimposed on basic states with gently sloped lower boundaries behaves similarly to that of the exact model at strong stratification.

The results corresponding to the exact model IL^∞ were derived starting from the primitive equations and restricting the analysis to strong shears (isopycnal slope much larger than that of the interface), e.g. $\bar{U}/U_\sigma \ll O(S^{-1})$ as $S \to 0$. The extension to weak shears is studied in Ripa (1997*b*), where a quasi-geostrophic reduced-gravity model is used from the beginning.

Useful discussions with W. R. Young, J. Sheinbaum and J. Ochoa are greatly appreciated. F.J.B.V. gratefully acknowledges the financial support provided by the Secretaría de Relaciones Exteriores del Gobierno de México in the form of an Argentina-México academic interchange's scholarship which made possible joining the M.S. program at C.I.C.E.S.E. This research has been supported by C.I.C.E.S.E.'s core funding and by C.O.N.A.C.yT. (México) under grant 1282-T9204.

Appendix A. Construction of the basic state

Consider the basic velocity written as

$$U(y,z) = \bar{U} + \left[1 + 2\frac{z}{H(y)}\right] U_\sigma \tag{A 1}$$

and the basic buoyancy as

$$\Theta(y,z) = \bar{\Theta}(y) + \left[1 + 2\frac{z}{H(y)}\right] \Theta_\sigma(y).$$

Integrating the hydrostatic balance up from the base of the active layer it follows that

$$P = \bar{\Theta} H + \left(\bar{\Theta} + \Theta_\sigma\right) z + \frac{\Theta_\sigma}{H} z^2.$$

Since there are no terms proportional to z^2 in (A 1), the geostrophic balance requires $\Theta_\sigma/H = \text{const.}$, say

$$\frac{\Theta_\sigma}{H} = \tfrac{1}{2} N_r^2.$$

Both coefficients of the linear profile in (A 1) yield, through the geostrophic balance,

$$f\left(\bar{U} + U_\sigma\right) + \frac{\mathrm{d}}{\mathrm{d}y}\left(\bar{\Theta} H\right) = 0, \quad 4f\frac{U_\sigma}{H} + 2\frac{\mathrm{d}\bar{\Theta}}{\mathrm{d}y} + N_r^2\frac{\mathrm{d}H}{\mathrm{d}y} = 0. \tag{A 2}$$

These equations are used to calculate $\bar{\Theta}(y)$ and $H(y)$.

Now, if it is assumed that

$$\bar{U}, U_\sigma \sim \varepsilon f L,$$

where L is a typical horizontal length scale and $\varepsilon \to 0$, then it follows that

$$\bar{\Theta} = g_r + Ay + O\left(\varepsilon^2\right) \quad \text{and} \quad H = H_r + By + O\left(\varepsilon^2\right),$$

where the coefficients A and B must be such that

$$\begin{pmatrix} f\left(\bar{U} + U_\sigma\right) \\ fU_\sigma \end{pmatrix} + \begin{pmatrix} H_r & g_r \\ H_r/2 & N_r^2 H_r/4 \end{pmatrix} \begin{pmatrix} A \\ B \end{pmatrix} = 0,$$

in order to satisfy (A 2). Hence, up to $O(\varepsilon)$, expressions (2.4)–(2.5) follow. □

Appendix B. Linearized bottom boundary condition

Taking into account that

$$P + ap' + O(a^2) = 0 \quad \text{at} \quad z = -\left[H + ah' + O(a^2)\right],$$

where $P(z = -H) = 0$, and expanding in Taylor series about $-H$, i.e.

$$a\left[p' - (\partial_z P)\, h'\right] + O(a^2) = 0 \quad \text{at} \quad z = -H,$$

it follows to $O(a)$ that

$$p' = \Theta h' \quad \text{at} \quad z = -H, \tag{B 1}$$

since $\partial_z P = \Theta$. In addition, the kinematic bottom boundary condition to $O(a)$ reads

$$w' = -\left(\partial_t h' + U\partial_x h' + \frac{fU}{\Theta} v'\right) \quad \text{at} \quad z = -H. \tag{B 2}$$

The bottom boundary condition (2.12) follows immediately after combining (B 1) and (B 2), but keeping only the lowest order in ε of the basic fields. □

Appendix C. Eigenvalue equation for the IL^1 model

Writing the system (3.21) in terms of the perturbation streamfunctions according to (2.13) and (2.16), and using (3.22) it follows that

$$\begin{pmatrix} 3\kappa_E^2\lambda + 3\dfrac{\lambda+\alpha}{1-S} & -\kappa_E^2 - 3\dfrac{\lambda+\alpha}{1-S} & \dfrac{\lambda+\alpha}{1-S} \\ 3S\dfrac{\lambda+\alpha}{1-S} + \kappa_E^2 S - 6 & 6\alpha - \kappa_E^2 S\lambda + 3(S-2)\dfrac{\lambda+\alpha}{1-S} & S\dfrac{\lambda+\alpha}{1-S} + 2 \\ -3S(\lambda+\alpha) & 3S(\lambda+\alpha) & (5S-6)\lambda - S \end{pmatrix} \begin{pmatrix} \bar{\psi}' \\ \psi'_\sigma \\ \psi'_{\sigma\sigma} \end{pmatrix} = 0,$$

where $\lambda := (c - \bar{U})/U_\sigma$ and $\alpha := \bar{U}/U_\sigma$. Non-trivial solutions will only exist if the determinant of the matrix vanishes, which results in a third-order algebraic eigenvalue equation, namely

$$C_1\lambda^3 + C_2\lambda^2 + C_3\lambda + C_4 = 0, \tag{C 1}$$

whose coefficients are given by

$$\begin{aligned} C_1 &= (1-S)\left[S(5S-6)\kappa_E^4 + 6(S-6)\kappa_E^2 - 36\right], \\ C_2 &= \left(S^3 - S^2\right)\kappa_E^4 + 4\left[(7\alpha-4)S + 3 - 6\alpha\right]S\kappa_E^2 + 6(5+7\alpha)S - 36(\alpha+1), \\ C_3 &= \left(\tfrac{5}{3}S^3 - \tfrac{11}{3}S^2 + 2S\right)\kappa_E^4 + \left[2\left(2\alpha^2 - 12\alpha - 3\right)S^2 + 2(9\alpha+10)S - 12\right]\kappa_E^2 \\ &\quad + 6\left(\alpha^2 + 6\alpha - 1\right)S - 36\alpha, \\ C_4 &= \tfrac{1}{3}\left(S^2 - S^3\right)\kappa_E^4 - \left[2\left(\alpha^2 - 2\alpha - 1\right)S + 2(\alpha+1)\right]\kappa_E^2 + 6\left(\alpha^2 - \alpha\right). \end{aligned}$$

REFERENCES

Farrell, B. F. 1982 The initial growth of disturbances in a baroclinic flow. *J. Atmos. Sci.* **39**, 1663–1684.

Fukamachi, Y., McCreary, J. & Proehl, J. 1995 Instability of density fronts in layer and continuously stratified models. *J. Geophys. Res.* **100**, 2559–2577 (referred to herein as FMP).

Gill, A. 1982 *Atmosphere-Ocean Dynamics*. Academic.

Pedlosky, J. 1987 *Geophysical Fluid Dynamics*. Springer.

Ripa, P. 1990 Positive, negative and zero wave energy, and the flow stability problem in the Eulerian and Lagrangian-Eulerian descriptions. *Pure Appl. Geophys.* **133**, 713–732.

Ripa, P. 1995 On improving a one-layer ocean model with thermodynamics. *J. Fluid Mech.* **303**, 169–201 (referred to herein as R95).

Ripa, P. 1996*a* Linear waves in a one-layer ocean model with thermodynamics. *J. Geophys. Res.* **101**, 1233–1245.

Ripa, P. 1996*b* Low-frequency approximation of a vertically averaged ocean model with thermodynamics. *Rev. Mex. Fís.* **42**, 117–135.

Ripa, P. 1997*a* A low-frequency one-layer model with variable stratification and vertical shear. *J. Fluid Mech.* (submitted) (referred to herein as R97).

Ripa, P. 1997*b* Baroclinic instability in a reduced gravity, three-dimensional, quasi-geostrophic model. *J. Fluid Mech.* (submitted).

Stone, P. 1966 On non-geostrophic baroclinic stability. *J. Atmos. Sci.* **23**, 390–400.

Stone, P. 1970 On non-geostrophic baroclinic stability, Part II. *J. Atmos. Sci.* **27**, 721–726.

Tandon, A. & Garret, C. 1995 Geostrophic adjustment and restratification of a mixed layer above a stratified layer. *J. Phys. Oceanogr.* **25**, 2229–2241.

Vanneste, J. 1993 The Kelvin–Helmholtz instability in a non-geostrophic baroclinic unstable flow. *Math. Comput. Modelling* **17**, 149–154.

Young, W. R. 1994 The subinertial mixed layer approximation. *J. Phys. Oceanogr.* **24**, 1812–1826.

Young, W. R. & Chen, L. 1995 Baroclinic instability and the thermohaline alignment in the mixed layer. *J. Phys. Oceanogr.* **25**, 3117–3185.